A Corrective Scheme to Prevent Adverse Dynamic Interaction of Grid-forming Inverters

Muhammad F. Umar[1], Mohsen Hosseinzadehtaher[1], Mohammad B. Shadmand[1], Hanif Livani[2], and Mohammed Ben-Idris[2]
[1]Intelligent Power Electronics at Grid Edge (IPEG) Research Laboratory, Department of Electrical & Computer Engineering, University of Illinois Chicago
[2]Department of Electrical and Biomedical Engineering, University of Nevada Reno
mumar6@uic.edu, mhosse5@uic.edu, shadmand@uic.edu, hlivani@unr.edu, mbenidris@unr.edu

***Abstract*— This paper proposes a control scheme that prevents the adverse dynamic interactions between the heterogeneously controlled grid-forming inverters (GFMI) in power electronics dominated grid (PEDG) towards a resilient self-driving grid. The primary controller of GFMIs in a grid cluster can vary based on their manufacturers such as virtual synchronous generation, droop control, power synchronization control, etc. Therefore, this can introduce heterogeneity among the network of GFMIs in PEDG. Resultantly, during the interconnection of GFMIs that are based on heterogenous primary controller poses various synchronization and dynamic interaction challenges in PEDG. For instance, severe fluctuations in frequency and voltage, high ROCOF, unintended reactive power circulation, etc. can occur. Therefore, to mitigate these adverse dynamic interactions among the GFMIs, a force enclaved homogenization (FEH) control is proposed in a supervisory level controller. This will autonomously adjust inertia coefficients of the each GFMI to have homogenous transient response and will enforce coherency among the heterogenous DGs. This will prevent the PEDG from the adverse dynamic interactions during an interconnection and load disturbance. Various case studies are presented that validates the proposed FEH control.**

Keywords— grid-forming inverter, virtual synchronous generator, homogeneous dynamic response, transient stability

I. Introduction

Integration of more renewable generation such as solar energy, and wind energy in the grid leads to rapid transition of the conventional power system from centralized generation towards more distributed generation. Higher penetration of renewable energy requires a power electronics interface such as inverter to control the generated power and meet the grid standards [1]. Thus, a new energy paradigm known as power electronics dominated grid (PEDG) that comprises higher number of power electronics based devices such as inverters are incorporated in the grid [2]. Broadly, based on the applications and control architecture the inverters are classified as grid-forming inverters (GFMIs) and grid-following inverters (GFLIs) [3]. The primary role of the GFMIs is to regulate the frequency and voltage of a network. However, in PEDG the GFMIs can perform various roles such as providing virtual inertia, grid voltage support, etc. Therefore, various control strategies to realize GFMIs are proposed in the literature.

Droop based control is widely applied approach for sharing the active and reactive power in the microgrid with several interconnected GFMIs [4, 5]. In [6], the classical droop control was modified to provide the improved reactive power sharing among the interconnected GFMIs. A derivative and integral term was added in the classical droop control to achieve this response. A reverse droop control is proposed in the [7] for the more resistive and lower X/R ratio networks. In [8], an adaptive droop based scheme is proposed for the non-linear and unbalanced loads in the system. The proposed control uses a combination of deadbeat and repetitive control to boost the performance of control under unbalanced and distorted loads.

Virtual synchronous generator (VSG) based control is another approach to realize the GFMIs that mimics the synchronous generator dynamics by employing the swing equation in the control loop of the VSG [9]. Moreover, this approach can provide a virtual inertia and improves the overall stability of the power system [10]. A comprehensive analysis of VSG for the applications in microgrid under harmonics and voltage suppression is presented in [11]. In [12, 13], a transient analysis of a microgrid comprised of the interconnected VSGs is presented. In these works, transient power oscillations are reported that are generated due to the inertia difference between the VSGs. Furthermore, to mitigate the stability issues of parallel operation of DGs based on VSG is presented in [14]. This scheme is based on utilizing the virtual impedance to provide the optimized inertia and damping ratios to avoid the oscillations in frequency and power. Although the proposed control schemes for GFMIs in the literature address various applications, however the missing piece of puzzle is the dynamic interaction analysis for the network of GFMIs with heterogeneous primary controllers. Specifically, the main challenge arises when the heterogeneously controlled GFMIs are interconnected during the clustering process [14]. Furthermore, the problem worsens since each GFMIs in the low-voltage distribution network may have different manufacturers, ratings, and filter sizes. Therefore, this will inherently bring non-homogeneity in the PEDG that results in adverse dynamic interactions during a disturbance or an interconnection process. The effects of adverse dynamic interactions includes high rate of change of frequency (ROCOF) that violates the maximum allowable ROCOF suggested by IEEE-1547-2018 standard [1]. Furthermore, the undesired reactive power circulation can occur during a disturbance [12] which easily disrupts the system stability and interconnected system may lose synchronism.

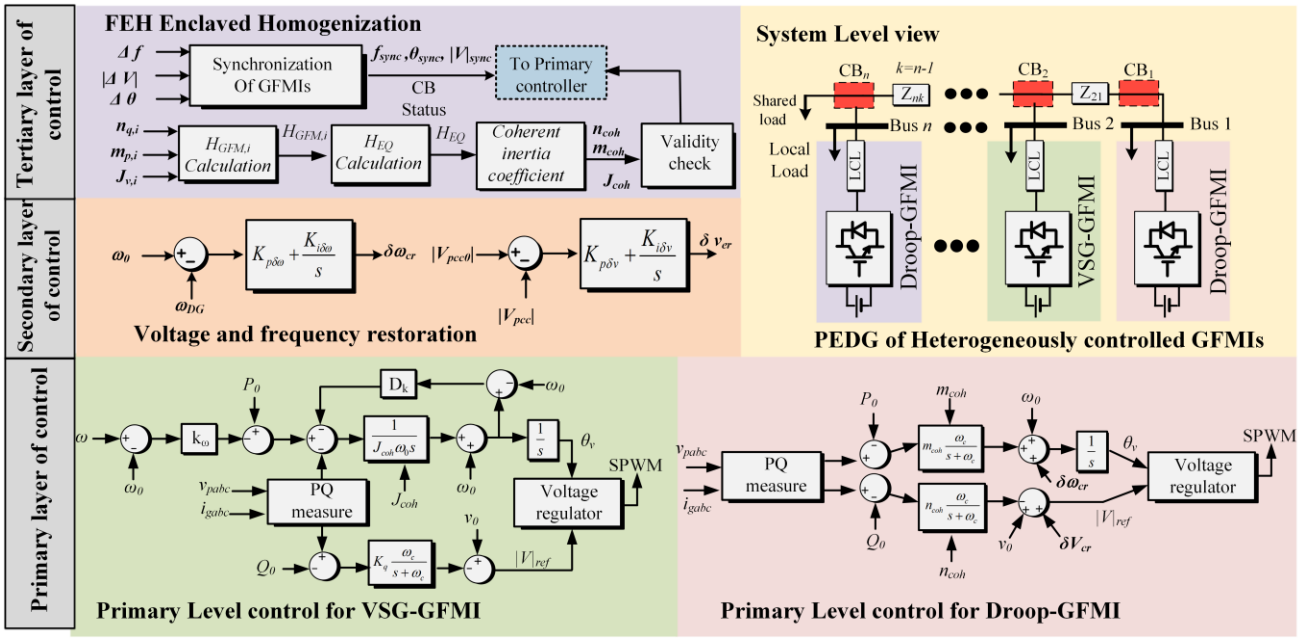

Fig. 1. Network of GFMIs with different primary control loops: VSG-GFMI and Droop-GFMI with a secondary voltage and frequency restoration control loop. Proposed coordinated controller for homogenization of GFMIs is shown as the tertiary layer of control that prevents the adverse dynamic interaction of GFMIs with different primary control loop and characteristics.

This paper proposes a forced enclaved homogenization (FEH) control methodology at supervisory level to prevent abovementioned adverse effects from dynamic interactions of heterogeneously controlled GFMIs. This is accomplished by autonomously adjusting the inertia coefficients of individual heterogeneous GFMIs towards self-driving future grid. Initially, the FEH control devise the system equivalent inertia by getting inputs from the primary controllers. Therefore, based on the equivalent inertia of the understudy PEDG, the gains for the primary controllers required to enforce homogeneity are derived. The coherent gains are then incorporated in the primary controller to adjust the system inertia, and this brings homogeneity in the transient response of all GFMIs and thus, prevents the PEDG from adverse dynamic interaction. Section II presents the mathematical modeling of the proposed three level controller. Section III provides an algorithm for the proposed control. Section IV discusses the obtained results. Lastly, the conclusion of the paper is presented in section V.

II. Mathematical Modeling of Proposed FEH control

The system description and structure of the proposed FEH control is illustrated by Fig. 1. The Fig.1 reveals that network of GFMIs has different primary controllers. For instance, $GFMI_1$ has droop-based primary controller whereas the $GFMI_2$ has VSG based primary control architecture. This pattern is repeated by n number of inverters with different power ratings and filter size. Thus, the considered system is heterogenous in nature. Furthermore, the proposed control structure is hierarchical and comprises primary level for the each GFMIs, secondary level control for the frequency and voltage restoration for droop based GFMIs and tertiary level control that includes cluster synchronization and proposed FEH.

A. Primary Controller

As shown in Fig.1, the considered PEDG has primary controller for each individual GFMIs with different structure. The governing equation for VSG based primary level controller is given by,

$$J\omega\frac{d\omega}{dt} = P_{nom} - P_m + D_k(\omega - \omega_0);\ \theta = \int \omega\, dt \tag{1}$$

$$v = k_q(Q_m - Q_{nom}) - v_0 \tag{2}$$

where, J is virtual inertia constant, P_{nom} and P_m are the nominal and measured active powers, ω and ω_0 are the instantaneous frequency and nominal frequency, D_k is the damping constant, θ refers to the voltage angle, v_o is the nominal RMS value of the voltage, Q_{nom} and Q_m refers to the nominal and measured reactive powers, and k_q refers to excitor constant. Moreover, the mathematical model of droop based GFMIs is given as,

$$\omega - \omega_0 = m_p(P_{nom} - P_f) \tag{3}$$

$$v - v_0 = n_q(Q_f - Q_{nom}) \tag{4}$$

where, m_p, n_q denotes the droop gains for the controller. Then, the voltage references generated by this primary level controller is given to the voltage regulation block to generate the appropriate SPWM signals for the three-phase inverter bridge.

B. Secondary Control

In the droop based GFMIs, the frequency and voltage are restored by utilizing a proportional integral (PI) secondary control. After the load disturbance in the droop control the voltage and frequency are shifted to lower or greater than

nominal values. The error between the nominal and measured values of the local PCC voltage and frequency of GFMIs is minimized by PI control and given as,

$$\delta\omega_{cr} = K_{p\delta\omega}(\omega_0 - \omega_{DG}) + K_{i\delta\omega}\int(\omega_0 - \omega_{DG})dt \quad (5)$$

$$\delta V_{pcc} = K_{p\delta v}(V_{pcc0} - V_{pcc}) + K_{i\delta v}\int(V_{pcc0} - V_{pcc})dt \quad (6)$$

where $\Delta\omega_{cr}$ is defined as error in the frequency and ΔV_{pcc} denotes error in the PCC voltage. $K_{p\delta\omega}$, $K_{i\delta\omega}$ are the proportional and integral gains for the frequency restoration approach. $K_{p\delta v}$ and $K_{i\delta v}$ are the proportional and integral gains for the V_{PCC} voltage restoration scheme. The secondary controller operates at 10 times slower rate than the primary controller of the GFMIs. Moreover, this error in frequency and voltage generated from the secondary control is feed forward in the droop controller loop to restore the voltage and frequency to the nominal values after the load disturbance. Thus, this control layer ensures that the droop based GFMIs have similar frequency and voltage restoration capability as the governor and excitor restores the frequency and voltage in the VSG.

C. *Proposed FEH control in Tertiary Control*

The proposed FEH scheme is based on the calculating the equivalent inertia constant H_{EQ} for the PEDG by leveraging the primary level controller's parameters of GFMIs. In the droop-based GFMIs, a low-pass filter in the active power control loop is emulating the virtual inertia [15] and the relation between the inertia constant and the droop gains is given by (7). Moreover, the inertia constant from the VSG based primary controller is given by (8).

$$H_{D,j} = \frac{1}{2m_{p,j}\omega_{c,i}} \;;\; D_{k,j}m_{p,j} = 1 \quad (7)$$

$$H_{v,i} = \frac{J_{v,i}\omega_0^{\,2}}{2S_{nom,i}} \quad (8)$$

where, $H_{D,j}$ is the inertia constant derived from the droop based controller, $H_{v,i}$ is the inertia constant calculated from the VSG based controller, $\omega_{c,i}$ refers to the cut-off frequency of the low-pass filter, $S_{nom,i}$ is the rated nominal power of a VSG based GFMI. Furthermore, the equivalent inertia of the PEDG is calculated by,

$$H_{EQ} = \frac{\sum_{k=1}^{n} H_k S_K}{S_{p,rated}} \quad (9)$$

where, S_k, and $S_{p,rated}$ refers to the individual nominal power and rated power of PEDG, respectively. H_k and H_{EQ} denotes the individual and equivalent inertia constant, respectively. Thus, the coherent gains for droop-based GFMI and coherent inertia constant for VSG-based GFMI is given by,

$$m_{coh,k} = \frac{1}{2H_{EQ}\omega_{c,k}} \quad (10)$$

$$J_{coh,i} = \frac{2H_{EQ}S_{nom,i}}{\omega_0^{\,2}} \quad (11)$$

where, $m_{coh,k}$ is the droop gain for the k_{th} GFMI based on the droop control and $J_{coh,i}$ is the virtual inertia constant for the i_{th} GFMI based on VSG. These modified droop and inertia coefficients are required to enforce the homogeneity among the cluster of heterogeneously controlled GFMIs. Finally, these coherent gains are incorporated in the primary controller of GFMIs as illustrated in Fig. 1.

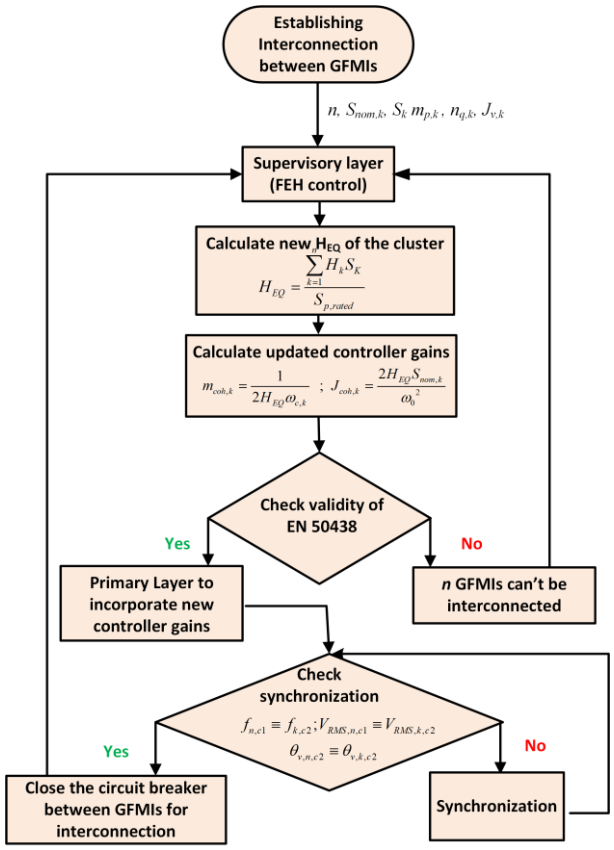

Fig.2 Algorithm flow chart for the interconnection of PEDG via proposed FEH.

III. Algorithm for Proposed Control

The interconnection algorithm based on the proposed FEH scheme for heterogeneously controlled GFMIs is illustrated in Fig. 2. Initially, the tertiary layer of control receives the information about GFMIs' power ratings, droop gains and virtual inertia constant from the primary controller. Based on this information each GFMIs' inertia contribution is calculated by using (7) and (8). Then, equivalent inertia coefficient based on the total power rating of the PEDG is determined by (9). leveraging the equivalent inertia coefficient coherent droop gain is calculated by (10). Moreover, for the VSG based GFMI the coherent virtual inertia constant is devised by using (11). The coherent droop gains are calculated for each GFMIs and validated for the compliance of the standard EN50438 [16]. If the coherent droop gains cannot satisfy the compliance test constraints, an error message is generated to show that GFMIs cannot be interconnected with existing PEDG. Otherwise, the coherent droop gains and coherent virtual inertia constant is passed to the primary layer of control for the incorporation into the control loop. Furthermore, the supervisory layer of control

TABLE I: SYSTEM SPECIFICATION

Parameter	Value
Rated Power of GFM_1, GFM_2, GFM_3	10,12,15 kW
L_{11}, L_{12}, L_{13}	1.2,1.5,1.8 mH
L_{21}, L_{22}, L_{23}	0.25,0.35,0.45 mH
C_{f1}, C_{f2}, C_{f3}	25, 35, 45 µF
m_2, m_3	(3.5, 5.5) x10^{-4}
J_1	0.016 kgm^2

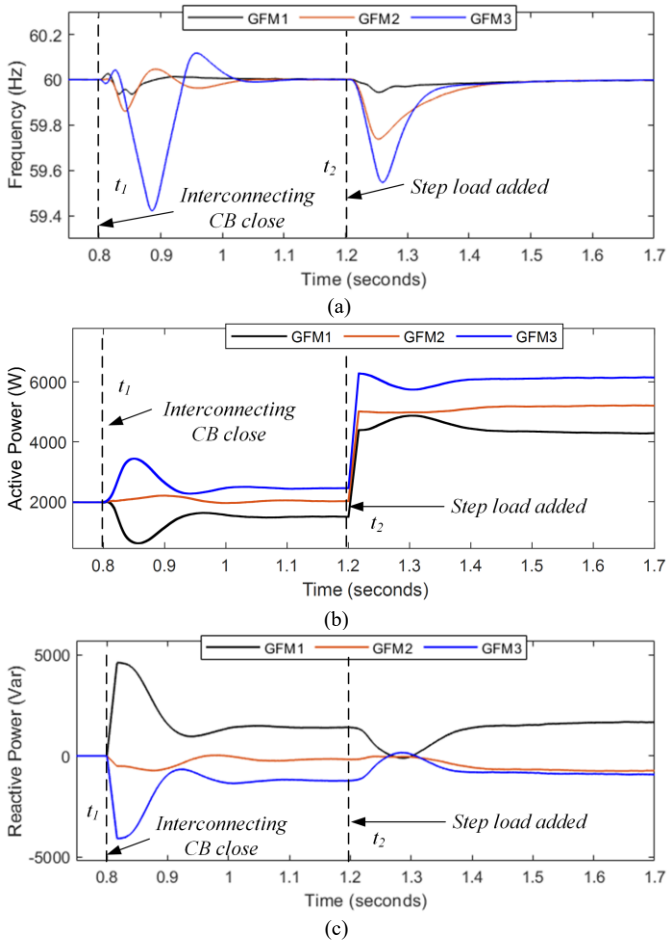

Fig. 3 Interconnecting heterogenous GFMIs based VSG and Droop control loops without proposed approach: (a) Frequency dynamic response, (b) Active power profile, (c) Reactive power profile.

checks the synchronization between the interconnecting GFMIs. The criteria of the synchronization scheme are based on checking the frequency, voltage angle and RMS of V_{PCC} of the interconnecting GFMIs. The supervisory layer of control commands the closing signal to the circuit breaker when the frequency, voltage angle and RMS of V_{PCC} of interconnecting GFMIs are within the accepted predefined thresholds. Otherwise, slight modifications are applied on the frequency, voltage angle and RMS of V_{PCC} till that time the error between the interconnecting GFMIs is within acceptable range. As soon as the error between the interconnecting GFMIs hits that range, the synchronization between the GFMIs is completed and the ON signal is given to the circuit breaker between the interconnecting GFMIs. Moreover, the addition of the small

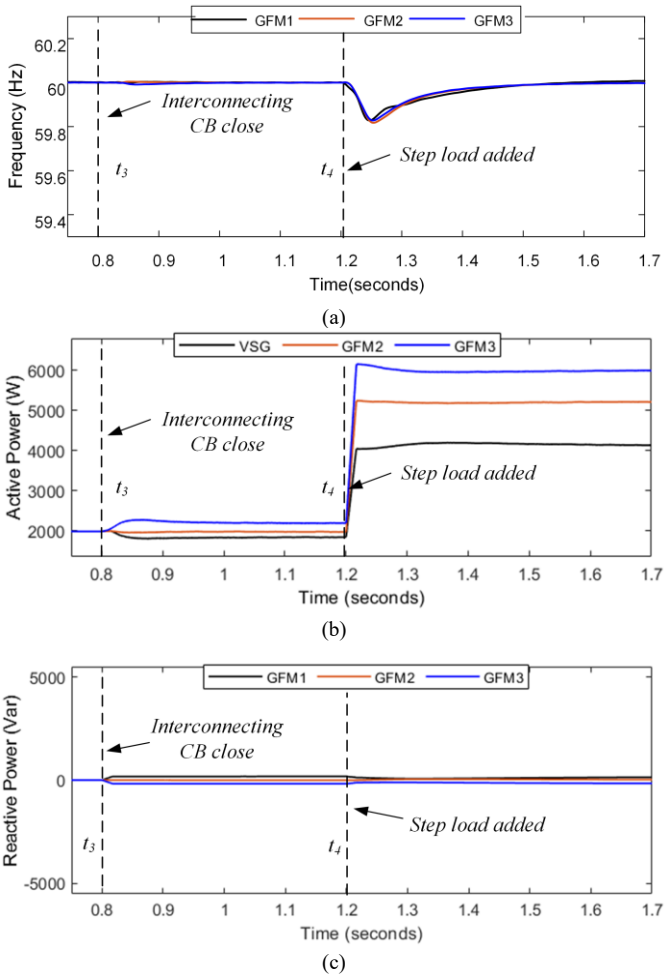

Fig. 4 Interconnecting heterogenous GFM with the proposed approach: (a) Frequency dynamic response, (b) Active power profile, (c) Reactive power profile.

step in the frequency, voltage angle and the RMS of V_{PCC} is halted. Thus, based on proposed control the adverse effects from the dynamic interactions of GFMIs are mitigated. The case studies related to the validation of the proposed control is given in the next section.

IV. RESULTS AND DISCUSSION

The developed FEH control was tested in a PEDG comprising three heterogeneously controlled GFMIs. The GFM_1 has a primary controller based on VSG while GFM_2 and GFM_3 have droop based primary controllers. The parameters for the simulation are given in Table I. Fig. 3 illustrates the interconnection of heterogeneous GFMIs without the proposed FEH control. The adverse effects of the dynamic interaction between the heterogeneous GFMIs are clearly seen in the Fig. 3. Specifically, at instant t_1 the circuit breaker (CB) between the three GFMIs is closed. Fig. 3(a) illustrates the adverse effects on the line frequency of the three GFMIs. High ROCOF is observed in the frequency of GFM_3, and a lower frequency nadir of 59.4 Hz is measured. The restoration of the frequency took almost 0.3s. Furthermore, at instant t_2 a step load of 15kw is added and a heterogeneous frequency dynamic response is

observed. Similarly, a high ROCOF and lower frequency nadir was observed for GFM_3. Fig. 3 (b) illustrates the active power profile of three GFMIs under the interconnection and addition of step load. Specifically, at instant t_1, the three GFMIs started sharing the active power. However, due to the heterogenous frequency dynamics, a non-favorable transient in the active power of GFMIs is seen. Moreover, an undesired reactive power was injected in the PEDG as shown in the Fig. 3 (b). This phenomenon is because the non-favorable transients in active power are impacting the V_{PCC} voltage of GFMIs and a mismatch between the V_{PCC} voltage occurred. Thus, it resulted in the undesired reactive power injection. Specifically, at instant t_1, GFM_1 starts injecting the reactive power that shoots to 4800 VAR initially. Moreover, the GFM_3 is absorbing the injected reactive power, thus it will lead to difference in power factor and terminal voltages of both GFMIs.

Comparatively, with the proposed FEH control the interconnection between three GFMIs is smooth and seamless. Fig. 4 (a) depicts the frequency of the GFMIs during the interconnection and addition of step load of 15kW. Specifically, at instant t_3, the signal of interconnection between the three GFMIs is triggered, and it can be seen in Fig.4 (a) that minimal disturbance in the line frequency is observed. Moreover, after addition of 15 kW load step, a homogeneous frequency dynamic response is seen because of enforced homogeneity among the three GFMIs. Fig. 4 (b) depicts the active power profile of GFMI with proposed control. At t_3, smooth active power sharing between the three GFMIs after the interconnection is measured. Furthermore, at instant t_4, after addition of 15kW load step a smooth power is shared between the three GFMIs. Fig.4(c) illustrates that negligible undesired reactive power is circulated and absorbed in the PEDG. Because of enforced homogeneity between three GFMIs the voltage unbalance didn't occur and resulted in negligible reactive power injection and absorption. Thus, with this case study it is validated that with proposed FEH the adverse dynamic effects between the interconnection of GFM with heterogenous primary controller are mitigated.

V. Conclustion

This paper presented FEH control scheme to avoid the adverse effects from the dynamic interactions between the GFMIs with heterogenous primary controllers. The proposed FEH control scheme forced the heterogeneous GFMIs to have the homogeneous frequency response during disturbance. Resultantly, a seamless interconnection between the three GFMIs happened. Furthermore, severe fluctuations in the frequency, PCC voltage and high ROCOF were avoided by leveraging the proposed approach towards a resilient self-driving future grid. Therefore, the adverse dynamic effects from the GFMIs interactions are mitigated. A comparative case study is presented in the paper that validates the effectiveness of the proposed approach and reveals its benefits.

Acknowledgment

This work was supported by the U.S. National Science Foundation under Grant ECCS-2114442. The statements made herein are solely the responsibility of the author.

Refrences

[1] "IEEE Standard for Interconnection and Interoperability of Distributed Energy Resources with Associated Electric Power Systems Interfaces," *IEEE Std 1547-2018 (Revision of IEEE Std 1547-2003),* pp. 1-138, 2018, doi: 10.1109/IEEESTD.2018.8332112.

[2] Q. Peng, Q. Jiang, Y. Yang, T. Liu, H. Wang, and F. Blaabjerg, "On the Stability of Power Electronics-Dominated Systems: Challenges and Potential Solutions," *IEEE Transactions on Industry Applications,* vol. 55, no. 6, pp. 7657-7670, 2019, doi: 10.1109/TIA.2019.2936788.

[3] Y. Li, Y. Gu, and T. Green, "Revisiting Grid-Forming and Grid-Following Inverters: A Duality Theory," *IEEE Transactions on Power Systems,* 2022.

[4] Q.-C. Zhong, "Robust droop controller for accurate proportional load sharing among inverters operated in parallel," *IEEE Transactions on industrial Electronics,* vol. 60, no. 4, pp. 1281-1290, 2011.

[5] C. Dou, Z. Zhang, D. Yue, and M. Song, "Improved droop control based on virtual impedance and virtual power source in low-voltage microgrid," *IET Gener. Transm. Distrib,* vol. 11, no. 4, pp. 1046-1054, 2017.

[6] J. M. Guerrero, L. G. De Vicuna, J. Matas, M. Castilla, and J. Miret, "A wireless controller to enhance dynamic performance of parallel inverters in distributed generation systems," *IEEE Transactions on power electronics,* vol. 19, no. 5, pp. 1205-1213, 2004.

[7] J. M. Guerrero, J. Matas, L. G. de Vicuna, M. Castilla, and J. Miret, "Decentralized control for parallel operation of distributed generation inverters using resistive output impedance," *IEEE Transactions on industrial electronics,* vol. 54, no. 2, pp. 994-1004, 2007.

[8] M. B. Delghavi and A. Yazdani, "Islanded-mode control of electronically coupled distributed-resource units under unbalanced and nonlinear load conditions," *IEEE Transactions on Power Delivery,* vol. 26, no. 2, pp. 661-673, 2010.

[9] M. Torres and L. A. Lopes, "Virtual synchronous generator control in autonomous wind-diesel power systems," in *2009 IEEE Electrical Power & Energy Conference (EPEC)*, 2009: IEEE, pp. 1-6.

[10] K. Sakimoto, Y. Miura, and T. Ise, "Stabilization of a power system with a distributed generator by a virtual synchronous generator function," in *8th International Conference on Power Electronics-ECCE Asia*, 2011: IEEE, pp. 1498-1505.

[11] Y. Dong, S. Ma, Z. Han, H. Dong, and X. Li, "A Comprehensive Virtual Synchronous Generator Control Strategy for Harmonic and Imbalance Voltage Suppression of Multi-Inverter Parallel Microgrid," *Electronics,* vol. 11, no. 3, p. 492, 2022.

[12] K. Shi, W. Song, H. Ge, P. Xu, Y. Yang, and F. Blaabjerg, "Transient analysis of microgrids with parallel synchronous generators and virtual synchronous generators," *IEEE Transactions on Energy Conversion,* vol. 35, no. 1, pp. 95-105, 2019.

[13] A. D. Paquette, M. J. Reno, R. G. Harley, and D. M. Divan, "Sharing transient loads: Causes of unequal transient load sharing in islanded microgrid operation," *IEEE Industry Applications Magazine,* vol. 20, no. 2, pp. 23-34, 2013.

[14] J. Liu, Y. Miura, H. Bevrani, and T. Ise, "Enhanced virtual synchronous generator control for parallel inverters in microgrids," *IEEE Transactions on Smart Grid,* vol. 8, no. 5, pp. 2268-2277, 2016.

[15] M. F. Umar, M. Hosseinzadehtaher, and M. B. Shadmand, "Homogeneity Realization for Cluster of Heterogeneous Grid-forming Inverters," in *2021 6th IEEE Workshop on the Electronic Grid (eGRID)*, 8-10 Nov. 2021 2021, pp. 01-06, doi: 10.1109/eGRID52793.2021.9662145.

[16] *Requirements for the Connection of Micro Generators in Parallel With Public Low-Voltage Distribution Networks,*, 2008. [Online]. Available: https://standards.iteh.ai/catalog/standards/clc/e5472dcd-5831-4f6d-b92a-1069c92911fa/en-50438-2007